Sodium Flux in *Necturus* Proximal Tubule under Voltage Clamp

KENNETH R. SPRING and CHARLES V. PAGANELLI

From the Department of Physiology, School of Medicine, State University of New York at Buffalo, Buffalo, New York 14214. Dr. Spring's present address is the Department of Physiology, Yale University School of Medicine, New Haven, Connecticut 06510.

ABSTRACT Na transport and electrical properties of *Necturus* renal proximal tubules were analyzed, in vivo, by a voltage clamp method which utilizes an axial electrode in the tubule lumen for passage of current and simultaneous determination of net fluid (or Na) flux by the split droplet method. When the average spontaneous transepithelial potential difference of −8 mv (lumen negative) was reduced to zero by current passage, net Na flux doubled from a mean of 107 to 227 pmoles/cm² per sec. The relationship between flux and potential over the range −25 to +10 mv was nonlinear, with flux equilibrium at −15 mv and droplet expansion at more negative values. Calculated Na permeability at flux equilibrium was 7.0×10^{-6} cm/sec. Voltage transients, similar to those caused by intraepithelial unstirred layers, were observed at the end of clamping periods. Tubular electrical resistance measured by brief square or triangle wave pulses (<100 msec) averaged 43 ohm cm². The epithelial current-voltage relationship was linear over the range −100 to +100 mv, but displayed marked hysteresis during low frequency (<0.04 Hz) triangle wave clamps. The low transepithelial resistance and large opposing unidirectional ion fluxes suggest that passive ionic movements occur across extracellular shunt pathways, while the voltage transients and current-voltage hysteresis are consistent with the development of a local osmotic gradient within epithelium.

INTRODUCTION

The electrical potential difference (PD) across proximal tubular epithelium of *Necturus* kidney is normally the only detectable driving force for passive, net, Na movement from extracellular fluid (ECF) to tubular lumen. The electrical properties of proximal tubules have been the subject of continued investigation since the first report of the presence of a PD across the tubular epithelium (1). Previous investigations indicate the desirability of producing controlled changes in the transepithelial electrochemical gradient to analyze tubular cell characteristics and to estimate the rate of active ion transport (2).

As a method of studying electrical properties and transport characteristics of the tubular epithelium, we have systematically altered transepithelial PD and simultaneously measured net fluid movement in lengths of *Necturus* proximal tubules, in vivo. The PD was altered by a voltage clamp technique, which involves passage of current through the epithelium from an axial electrode placed in the lumen of the tubule, and the rate of fluid movement was simultaneously determined by the split droplet method. We have used the voltage clamp technique to: (*a*) estimate the rate of Na transport in the absence of a transepithelial PD, and compare this flux with that calculated from the simultaneously obtained short-circuit current (SCC); (*b*) establish the relationship between rate of fluid movement and transepithelial PD; (*c*) estimate the open circuit unidirectional fluxes and tubular Na permeability; (*d*) characterize the transepithelial resistance measured both instantaneously and under steady-state conditions.

METHODS

The experimental procedure was to inject large droplets of *Necturus* Ringer solution into long, straight, oil-filled segments of the proximal tubule, in vivo, and to place within those droplets both an axial current electrode and a glass microelectrode for recording transepithelial PD. The axial electrode was advanced into the droplet through the barrel of a sharpened micropipette (O.D. 25–30 μm), as shown in Fig. 1. Guard electrodes normally used in voltage clamp experiments were obviated because of the presence of insulating columns of oil which delimit a droplet of Ringer solution within the tubular lumen. Current flow was primarily restricted to the area containing Ringer solution, and complex electrical fields at the ends of the axial wire were avoided. The indifferent electrode for the current circuit, a platinum black, silver, silver chloride electrode lying under the kidney, was made as large as possible to aid in the development of a uniform electrical field. The transepithelial PD was clamped to a desired value by passage of an appropriate current through the wire, while salt and water reabsorption was measured simultaneously by direct microscopic observation of the change in length of the droplet of Ringer solution contained between the oil columns.

Adult *Necturus maculosus* of both sexes were obtained from Lemberger Co., Oshkosh, Wis., and stored at 15°C in a 30 gallon (100 liter) aquarium with rocks and cement blocks as shelters. They were anesthetized by immersion in a 0.1% tricaine methane sulfonate solution (Ayerst Laboratories, New York) at pH 4.5 and 15°C until skin reflexes disappeared. After removal from the anesthetic, they were washed in tap water and placed supine in a shallow trough on a table specially equipped for control of body temperature and ventilation of skin and gills (Fig. 2). The trough deepened gradually from about 1 cm in the area of the animal's body to 2 cm in the gill and head area. Cork surfaces on each side of the trough permitted fixing of the limbs by means of small pin clips. Water at 10°C flowed through the trough from the head toward the tail of the animal at rates from 15 to 50 cc/min. Intraperitoneal temperature, recorded during all experiments by means of a thermocouple attached

to the input of a Yellow Springs Instrument Company (Yellow Springs, Ohio) telethermometer, was maintained at 14° ± 1°C.

Howell et al. (3) have shown that the arterial pH of cold-blooded vertebrates decreases with increases in environmental temperature. To establish the effect of temperature on the pH of the animal's blood six unanesthetized *Necturus* were stored first at 10°C and later at 25°C for periods of 1 wk or more at each temperature. Mixed venous blood samples were obtained by heart puncture at each temperature and pH was determined at the appropriate temperature for each sample. These samples had an average pH of 7.834 at 10°C and 7.676 at 25°C. $\Delta pH/\Delta T$ was

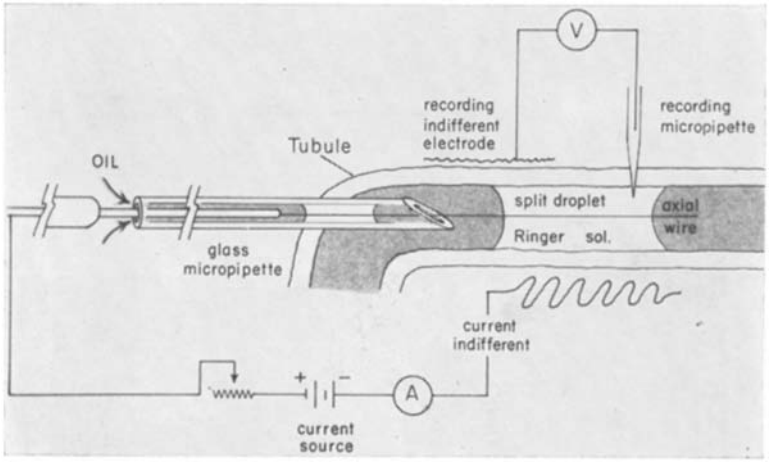

FIGURE. 1 Electrode arrangement for voltage clamping of a proximal tubular segment. The variable resistor in the circuit is used to control the current so that the potential difference is held at the desired value. The current indifferent electrode is a large platinized wire lying under the kidney; the current is displayed on an ammeter (*A*). The axial wire is moved hydraulically across the droplet, and additional droplets may be injected from the micropipette after reabsorption occurs. The voltage-recording electrode is a 3 M KCl–filled glass micropipette; the recording indifferent electrode is a saline-soaked wick in contact with a calomel cell. *V* represents an electrometer-voltmeter-oscilloscope combination.

−0.011; thus, animals maintained at 15°C should have a pH of about 7.78. Venous pH of anesthetized animals placed on the temperature-controlled table, evaluated in several micropuncture experiments lasting as long as 10 hr, was found to remain near 7.8. Renal blood flow was vigorous throughout the experiments, with little tendency toward vascular stasis.

The kidney was exposed for micropuncture in the manner described by Windhager (4), and illuminated with a fiber optic light pipe with a tungsten halide light source (Dolan-Jenner Industries, Inc., Melrose, Mass.). Micropuncture was carried out with the aid of a stereozoom research microscope (Bausch and Lomb Inc., Rochester, N. Y.), under 30–60 magnification. Fluid reabsorption was measured by the split droplet method of Gertz (5) as modified by Bentzel et al. (6). The Ringer

solution used for tubular perfusion and for bathing the renal surface was the same as that suggested by Giebisch (7), except that it was glucose free and the pH was adjusted to 7.8.

Potential differences were recorded by means of glass microelectrodes pulled to a

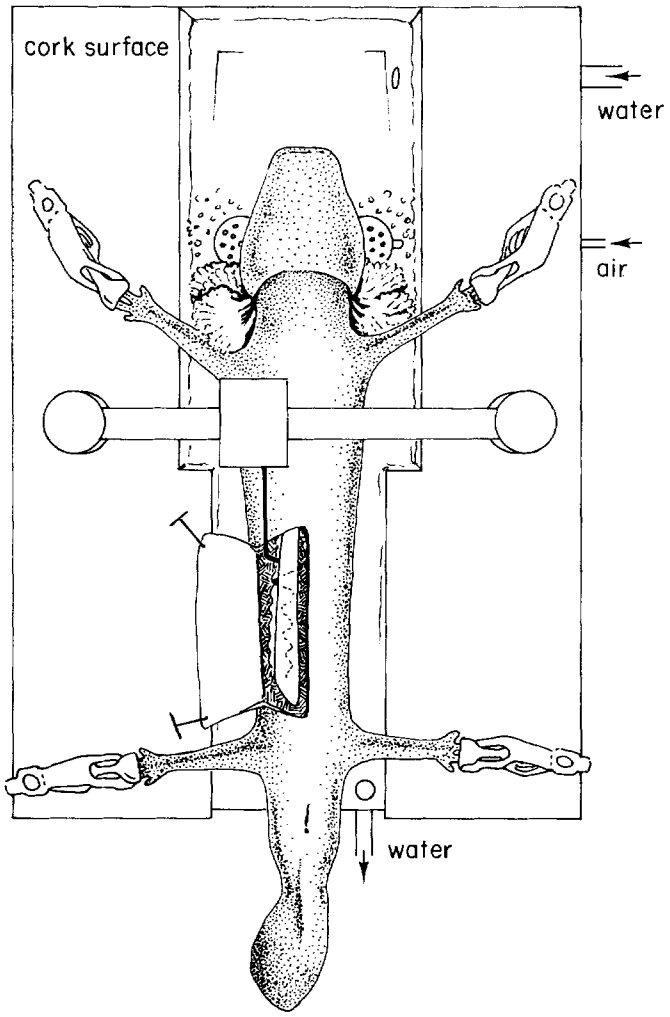

FIGURE 2. *Necturus* prepared for kidney micropuncture. Flowing water completely covers the animal's head and gills and the dorsal half of its body.

tip diameter of less than 1 μm and filled with either 3 M KCl or 1 M NaCl. Acceptable electrodes had impedances of 10–40 MΩ, and tip junction potentials of less than 5 mv. The microelectrode was connected through a calomel half cell to the probe input of a WPI electrometer (Model M-4, input $>10^{10}$ Ω, W-P Instruments, Inc., Hamden, Conn.) and the reference cell (a wick calomel electrode on the renal sur-

face) was connected to a variable-polarity compensation box, which permitted nulling of asymmetry potentials between electrodes as well as the tip junction potentials. The output of the electrometer was displayed both on a Tektronix 503 oscilloscope (Tektronix, Inc., Beaverton, Ore.) and a Fluke 854A voltmeter (John Fluke Mfg. Co., Inc., Seattle, Wash.). The oscilloscope was used to monitor impedance changes continuously in the recording electrode; impedance changes gave an indication of electrode condition and position as the electrode was advanced through the tubule wall and into the lumen. When the recording electrode was on the surface of the kidney, its impedance was on the order of 10–40 MΩ. Penetration of the electrode into an oil-filled tubular lumen resulted in an abrupt, five- to tenfold increase in impedance. When the oil was displaced by a droplet of Ringer solution, electrode impedance fell immediately to the original value. Any microelectrode insertion which did not exhibit this pattern of impedance change was considered unacceptable and another insertion was attempted. Peritubular membrane potentials less than 40 mv were rejected on the assumption that depolarization had occurred during electrode insertion. Tubular voltages were recorded by feeding the output of the voltmeter into one channel of a three-channel pen recorder.

The axial current electrode was a platinized tungsten wire 5–10 μm in diameter which was connected through a variable resistance to a source of direct current. The current record was displayed on the second channel of the pen recorder. The axial wire was inserted into the tubular lumen by means of the apparatus described below. Briefly, this apparatus permitted placement of an axial wire in the barrel of the tubular micropipette, and the smooth hydraulic advancement of that wire into the tubular lumen after puncture had been accomplished.

The apparatus for wire insertion (Fig. 3) consisted of two separable units: an anterior chamber, which was used to inject solutions through the micropipette, and a posterior chamber, a modified syringe, which was used to move the axial wire hydraulically. The anterior chamber, with a female Luer connector at one end and a pipette chuck at the other, was filled with 300 cp mineral oil and connected through a side arm to a 20 cc syringe. Pressure applied to the syringe resulted in injection of oil from the pipette tip or injection of a droplet of Ringer solution that had been drawn into the pipette prior to its insertion into the tubular lumen. The posterior chamber was a precision-fit 5 cc syringe with the following modifications: a side arm, soldered to the base of the syringe tip, was connected with polyethylene tubing to a 2 cc syringe, and the entire system was filled with 300 cp mineral oil. The 5 cc syringe plunger was drilled out to receive a 14 cm length of 0.72 mm diameter stainless steel tubing, which was cemented to the plunger with 6 cm extending beyond the forward end of the plunger. An O ring fitting in the syringe tip allowed the tubing to move in and out freely with the plunger, but prevented the escape of mineral oil from the 5 cc syringe. The O ring also prevented the movement of oil from anterior to posterior chamber when the apparatus was assembled. The tubing acted as a guide for the holder of the axial wire. It had a slightly tapered tip which seated in the lumen of the shaft of the glass micropipette. Electrical connections were made at the rear of the tubing.

A 22 cm length of 0.315 mm diameter tubing with a 0.13 mm diameter stainless pin soldered into the anterior end and a short length of polyethylene tubing on the

posterior end was slid inside the 0.72 mm tube. The pin fitting enabled easy replacement of wires; the platinized wire, soldered into a short length of 0.315 mm tubing, slipped snugly onto the pin. The polyethylene tube sealed the posterior end of the 0.72 mm tube, and prevented reflux of oil from the anterior chamber through this tube.

The axial electrode was made from a 2 cm length of 5–10 μm diameter tungsten wire[1] soldered into a 1 cm piece of 0.315 mm diameter stainless tubing and platinized by a modification of the method of Cole and Kishimoto (8). The wire was washed in distilled water, 70% ethanol, concentrated nitric acid, once again in distilled water, and finally placed in a Kohlrausch salt solution.[2] It was connected to the cathode of a Grass SD5 stimulator (Grass Instrument Co., Quincy, Mass.), and a

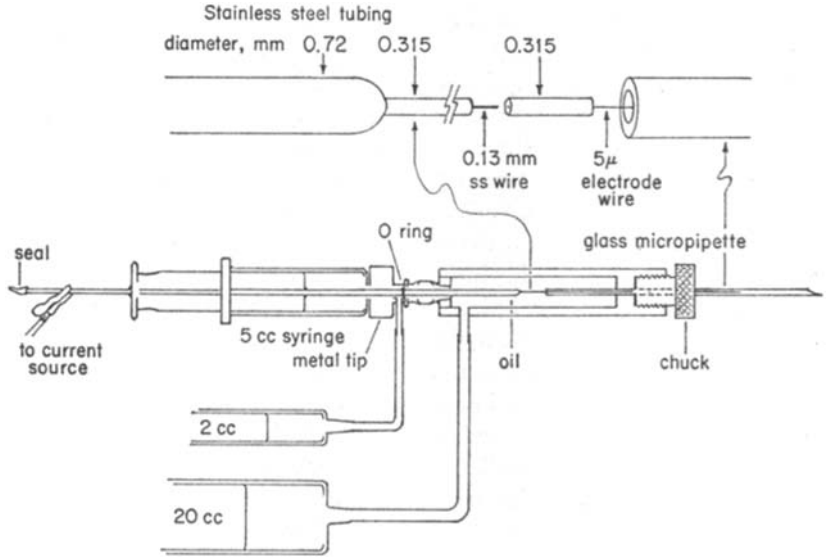

FIGURE 3. Apparatus used for electrode insertion. See text for detailed discussion.

clean platinum wire was used as the anode. Plating was carried out at a current density of 30 ma/cm^2 until about 1 coul/cm^2 had been passed. We typically used monophasic pulses of 10 msec duration and 4.0 v amplitude at a frequency of 30–40 pulses/sec for 60–120 sec. The tungsten wire then displayed a dull, gray coating of platinum black with a slight increase in diameter (8–12 μm total diameter).

The voltage difference between the wire electrode and a third electrode (a heavily platinized platinum wire) in the plating bath may be used continuously to monitor the electrical properties of the axial electrode (9). Plating was considered complete when the electrode's impedance, measured 1 msec after the beginning of each plating pulse, was no more than 25% greater than the initial resistance (usually about 125 Ω/cm). Although platinized wires are polarizable to a small extent, we found little evidence of significant polarization in vivo or in vitro. Undoubtedly the low

[1] General Electric Co., Tungsten Process, Cleveland Wire Plant, Cleveland, Ohio.

[2] 3% platinic chloride, 0.025% lead acetate, 0.025 N hydrochloric acid.

current densities required (<1 ma/cm² of wire) and the relatively high resistance of the epithelium minimize detectable polarization, since the resistance of the wire and surrounding fluid are less than 5% of the effective epithelial resistance. Platinized electrodes may also cause pH shifts or the generation of gas (hydrogen, oxygen, or chlorine). Gas generation, which may damage the tubule and prevent accurate determination of split droplet volume, was avoided by preventing contact of the wire with the tubular epithelium and by keeping the source voltage below 2 v.

Measurements of current-induced pH changes were made by inserting the axial electrode into the lumen of a 100 μm diameter, constant bore, glass capillary tube, filled with Ringer solution and bromcresol purple. The pH of this solution was adjusted to 7.8, and the end point for color change was determined by titration to be about pH 7.3. Continuous current passage for 10 min at 2×10^{-7} amp resulted in a pH shift of about 0.5 unit in this system.

The source voltage necessary to pass currents of up to 2×10^{-7} amp was generally 1 v or less. Occasionally currents were observed which were exceptionally high for a given change in transepithelial PD. Such high currents could usually be reduced by a slight repositioning of the wire and were attributed to shorting caused by contact between the axial electrode and the microvilli of the tubular cells, especially in the immediate vicinity of the puncture site.

The axial electrode was inserted into the tubule after a droplet of perfusate had been injected and the recording microelectrode was in place. Care was taken to prevent contact of the axial wire with the tubular wall to prevent damage to the tubular cells. Such damage was usually evidenced by a rapid leakage of fluid out of the lumen. Control measurements of fluid reabsorption were made before voltage clamping began, and then current was passed until the transepithelial PD was clamped to the desired value. The PD was held constant by manual adjustment of the current source.

Transepithelial resistance measurements were made with a conventional voltage clamp circuit (9). A differential, high input impedance, capacitance-compensated amplifier (Transidyne MPA-6, Transidyne General Corp., Ann Arbor, Mich.) received inputs from the voltage-recording and indifferent electrodes. The axial wire current electrode was connected to the output of an operational amplifier (Philbrick 1024, Philbrick/Nexus Research, Boston, Mass.) which served as the control amplifier. The current indifferent electrode was held at virtual ground by two stages of amplification (Philbrick SQ10A, Philbrick/Nexus Research), which also served to amplify the current signal 1000 times. The rise time of the voltage clamp system with a 20 MΩ microelectrode in place was about 125 μsec; the clamp had a gain of 10,000. Triangle waves of low frequency (<1000 Hz, Model 202A Low Frequency Function Generator, Hewlett Packard Co., Colorado Springs, Colo.) or square waves (SD-5 stimulator, Grass Instrument Co.) were used as command inputs to the summing junction of the control amplifier. The voltage and current records were displayed on a dual beam storage oscilloscope (Tektronix 564B, Tektronix, Inc.), monitored on voltmeters (Fluke 854A, John Fluke Mfg. Co., Inc.), and recorded on a multichannel pen writer (Brush Recorder Mark 260, Gould, Inc., Cleveland, Ohio).

Determination of the length of injected droplets was made continuously at mag-

nification 60 with the aid of an ocular micrometer disc. The smallest change in length which could be detected with certainty was about 15 μm. Changes in droplet size were recorded on the third channel of the pen writer as changes in the ratio of length measured from the ends of each oil column at any time $[L(t)]$ to length at initial observation $[L(0)]$. Half times ($t_{1/2}$) or doubling times (t_2) of droplets were determined by plotting the logarithm of droplet length after individual meniscus correction against time, as suggested by Nakajima et al. (10). Volume flux per unit area was converted to Na flux per unit area (J_{Na}) with the assumption of isosmotic fluid transport and a luminal Na concentration of 0.1 M/liter. Sodium permeability for passive flux from plasma to lumen was calculated using the equation developed by Goldman (11), as modified by Hodgkin and Katz (12).

RESULTS

Insertion of a microelectrode into the tubular wall resulted in a characteristic, negative intracellular PD; penetration into the lumen permitted measurement of a transepithelial PD, normally negative when tubular lumen is referred to the ECF. Intracellular PDs of proximal tubular cells are presented in Table I together with transepithelial PDs in free-flow and split droplet conditions. In a freely flowing tubule, measurement of transepithelial PD is complicated by inability to locate the electrode tip. Impedance monitoring, used to confirm the location of the electrode in an injected droplet, may also be carried out in free-flow measurements, but can only be used to ascertain whether the electrode tip has become occluded or broken in the course of transepithelial insertion. Split droplet PDs may therefore be regarded with greater confidence, since they represent records in which the electrode tip location was confirmed by the impedance monitoring technique previously described. The mean values for the free-flow and split droplet transepithelial PDs are significantly different. Whether this discrepancy is caused by measurement procedures, such as flow potentials or electrode position, or represents a true difference in tubular PD, is unknown at present.

Eight proximal tubules in different animals were punctured and droplets injected to provide a group of control observations. The mean half time for droplet shrinkage in this control group was not significantly different from those obtained by other investigators (13, 14), nor did it differ significantly from the mean value obtained with droplets in which both an axial wire and recording microelectrode were present (Table II). Accordingly, these values were pooled and treated as the control group of observations.[3] Current was passed in a tubule only after the axial wire and recording microelectrode were in place, and an adequate control record of shrinkage rate and spontaneous PD had been obtained. Current flow (axial wire positive with respect to the

[3] The pooled control droplets had the following dimensions: diameter, 110 ± 17 μm (mean ± SD); initial length, 488 ± 255 μm (mean ± SD); initial surface area, 18×10^{-4} cm^2; initial volume, 49.5×10^{-7} cm^3.

ECF) was used to reduce the transepithelial PD to zero, that is, to produce a so-called short circuit. The fluid transport rate increased substantially when the PD was eliminated; an example of this phenomenon is seen in Fig. 4. Mean droplet shrinkage rate in short-circuited droplets was more than double the rate in the open-circuit droplets (Table II). Calculated net sodium flux is also presented in Table II. Elimination of the transepithelial PD removes

TABLE I
ELECTRICAL POTENTIAL DIFFERENCES

Site of measurement	Number of observations	PD	
		mv	
Intracellular	198	−62.7±11.5*	
Transepithelial (free flow)	52	−12.6±6.5	$P<0.001$
Transepithelial (split droplet)	62	−8.1±4.3	

Electrical potential differences were measured with 3 M KCl-filled glass microelectrodes in the same group of animals used in the voltage clamp experiments.
* Mean ± SD.

TABLE II
VOLUME CHANGE OF SPLIT DROPLET

	No. of observations	Half time	Sodium flux	
		min	*pmoles/cm² per sec*	
Control I (no wire or electrode)	8	29.5±7.2*		$P>0.6$
Control II (wire and electrode)	20	31.4±10.1		
Pooled control	28	30.9±8.8	107±26.8	$P<0.001$
Short circuited	15	13.7±2.4	227±41.8	

* Mean ± SD.

the electrical driving force for net passive movement of Na from interstitial fluid to tubular lumen, and the observed fluid efflux results from active transport only. If it is assumed that active transport rate remains unchanged over the range of PD from 0 to −8 mv (the average open-circuit PD), then it is possible to determine the passive plasma-to-lumen flux by subtraction of the observed fluxes in the short-circuit and open-circuit states. In Table III, the fluxes measured in the present study are compared with those determined by Oken et al. (15), using radioisotopic tracers, by Eigler (16), using point-source short circuiting, and Boulpaep (17), using the expanding drop method.

The electrical short-circuit current (SCC) tended to decline as the droplet volume decreased because of the decrease in surface area and increases in

apparent transepithelial resistance (Fig. 5). To compare SCC with observed flux, it is necessary to integrate the current over time to obtain the net charge transfer and compare it with the total Na flux over the same time period. In four of the short-circuiting experiments, net electrical charge transfer was three or more times greater than sodium flux calculated from volume change, and these results were not averaged with the others. The large discrepancies between electrically measured charge transfers and those calculated from fluid

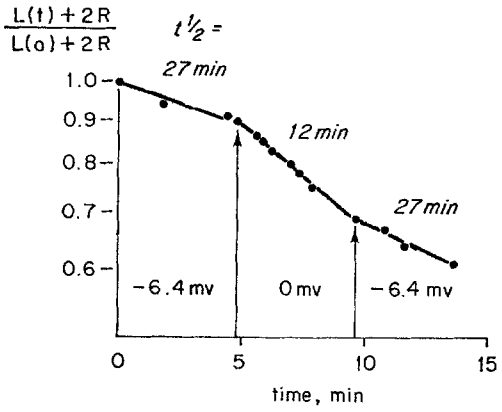

FIGURE 4

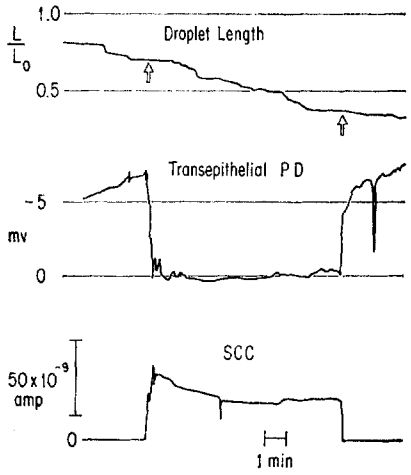

FIGURE 5

FIGURE 4. Rate of shrinkage of a single droplet in open and short-circuit conditions. Ordinate shows the logarithm of relative droplet length after correction for the fluid in the meniscus. The half time for reabsorption and transepithelial PD are shown in each section of the curve.

FIGURE 5. Record of short-circuiting experiment. The top trace is the ratio of the length of the droplet divided by its initial length, without any correction for meniscus. The second trace is the transepithelial PD, and the third is the current necessary to reduce the transepithelial PD to zero. At the points indicated by the vertical arrows current was turned on and off.

reabsorption are thought to be the consequence of shorting of the axial wire to microvilli. The results presented in Table IV show that net electrical charge transfer (ΔQ), calculated from SCC integrated over time, was not significantly different from the net Na charge transfer during that same time period, in part because variability of the electrical SCC was large. For each experiment, the total electrical and partial sodium conductances (G) were also calculated by dividing the respective SCC by the PD for that observation.

In addition to short-circuiting experiments, tubules were held at potentials ranging from -25 to $+10$ mv (luminal PD with respect to ECF) in 5-mv increments. Whenever possible, a single droplet was clamped to several differ-

ent PDs. Control periods were alternated with periods of voltage clamping as a check on the condition of the tubule. Droplet shrinkage rate and PD after release of the clamp were compared with the values obtained prior to clamping, and if serious discrepancies occurred, the experimental results were discarded. Fig. 6 illustrates a portion of an experiment in which a single droplet was clamped to seven different PDs, with no evidence of deterioration of spontaneous PD or spontaneous droplet shrinkage rate. When the PD was

TABLE III
SODIUM FLUX

	This study	Oken et al. (15)	Eigler (16)	Boulpaep (17)
Net flux	107±27*	62±41*	46±17*	165±178*
Active (lumen to plasma)	227±42	249±139		352±215
Passive (plasma to lumen)	120±49	187±133		187±119

Unidirectional sodium fluxes, determined from the data of Table II, are given in picomoles per square centimeter per second for an open-circuit tubule.
* Mean ± SD.

TABLE IV
COMPARISON OF ELECTRICAL CHARGE TRANSFER AND CURRENT WITH VALUES CALCULATED FROM NET OBSERVED DROPLET VOLUME CHANGE DURING THE SAME TIME PERIOD

	PD	ΔQ	SCC	G
	mv	*coul* × 10^{-8}	*μamp/cm²*	*mmho/cm²*
Current passed	−5.5±1.6*	1.42±0.58*	35.8±23.0*	6.2±2.4*
Na flux (from volume change)		1.25±0.6	22.8± 3.8	4.5±1.8
Ratio		1.14	1.57	1.38
		$P>0.1$	$P>0.1$	$P>0.1$

* Mean ± SD.

−15 mv, no net fluid movement occurred; at a PD of −20 mv, passive Na influx exceeded active efflux and the droplet expanded. Droplets were clamped to different PDs in a random sequence and were checked for deterioration of function by periodic release of the clamp. In more than 30 additional experiments, droplets could be clamped to only one or two different PDs before the experiments were interrupted by animal movement, vibrations in the laboratory which caused electrode displacement, total reabsorption of the droplet, or change in the position of the droplet. The changes in rate of droplet shrinkage or expansion produced by voltage-clamping were completely reversible, with return to control flux rate and transepithelial PD

on release of the clamp. Voltage transients typical of those seen in relaxation of concentration gradients in unstirred layers (18) were often observed after release of the clamp. These transients were most evident when the transepithelial PD was large (negative or positive) and usually disappeared with a half time of 1 min or less (Fig. 7).

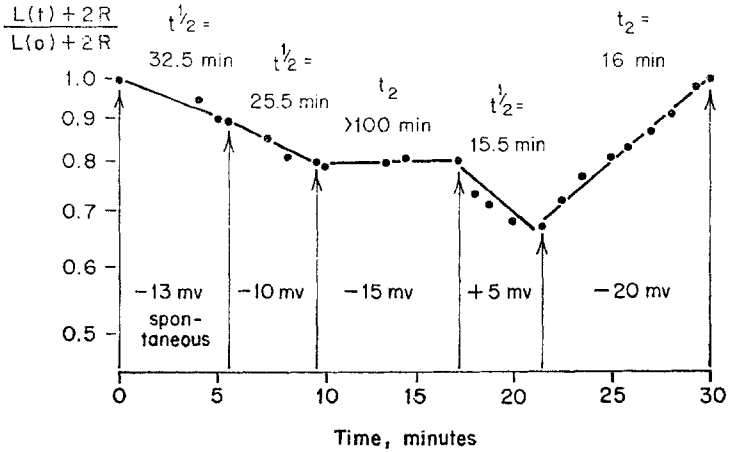

FIGURE 6. Rate of droplet shrinkage under control (spontaneous PD) and voltage clamp conditions. Ordinate is a logarithmic scale of relative droplet length after correction for the meniscus. In each panel, the half time ($t_{1/2}$) or doubling time (t_2) is shown above the line and the transepithelial PD to which the droplet was clamped is indicated below.

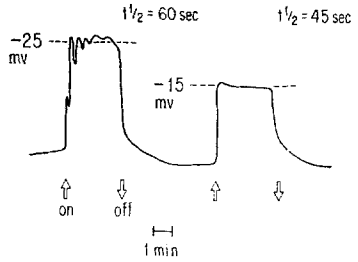

FIGURE 7. An example of the transepithelial voltage transients which follow the cessation of current passage. Current passage began at the point on the left indicated by the vertical arrow and ended at the arrow on the right. The $t_{1/2}$ for decay of the voltage transient is indicated above the record.

The pooled results of all voltage clamp experiments are presented in Fig. 8, in which net Na flux, calculated from the observed rate of fluid movement, is shown as a function of the clamped transepithelial PD. Two linear least squares lines were fitted to the data. The slope of the line from −15 to +10 mv was −15.2 ± 0.089 (SEM) pmoles/cm² per sec per mv, and the line from

−25 to −15 mv had a slope of −49.2 ± 0.25 (SEM) pmoles/cm² per sec per mv. Transepithelial Na permeability was calculated from the slope of the least squares line by the application of the Goldman-Hodgkin-Katz equation and the assumption of a constant active transport rate (equal to that observed under short-circuit conditions) at various PDs. In Table V, Na permeabilities

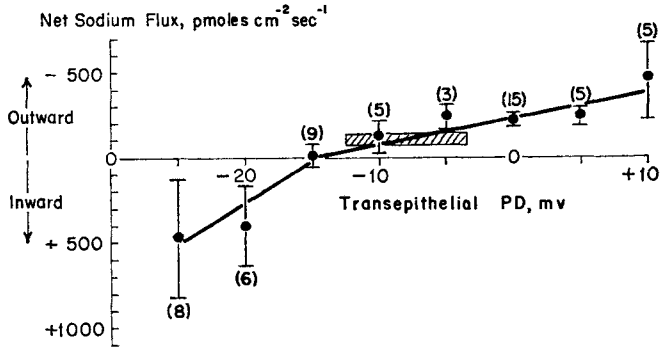

FIGURE 8. Net sodium flux as a function of transepithelial PD. Net outward flux (lumen to plasma) is represented by points above the abscissa, net inward flux (plasma to lumen) by points below the abscissa. The mean and standard deviation of the net flux are indicated for each PD (number of observations in parentheses) to which droplets were voltage clamped. The cross-hatched area depicts the mean ± 1 SD of the pooled control flux and potential. The data are fitted by two least squares lines.

TABLE V
SODIUM PERMEABILITY

	Sodium permeability
	× 10^{-6} cm/sec
Linear least squares (−15 to +10 mv)	3.73
Flux equilibrium (−15 mv)	7.05
Whittembury et al. (19)	
In situ	1.4
Slices	0.87
Boulpaep (17)	3.04

Sodium permeability was calculated from the data presented in Fig. 8, as discussed in the text.

so obtained are compared with those determined by Whittembury et al. (19) and Boulpaep (17).

Variability of droplet shrinkage rate increased substantially at transepithelial PDs more negative than −15 mv, even though all droplets clamped to potentials in this range exhibited flux reversal and expansion. The slope of the line in the region of droplet expansion suggests that an approximately

threefold increase in Na permeability may occur in tubules in which the injected droplet is expanding.

Transepithelial resistance determined from the current required for brief (up to 100 msec) step changes in transepithelial PD of up to 100 mv above or below the spontaneous PD did not exhibit time- or voltage-dependent changes. Current-voltage plots of transepithelial response to triangle wave voltage commands were linear at frequencies between 10 and 100 Hz. Triangle wave commands of very low frequency (less than 0.04 Hz) resulted in marked hysteresis (Fig. 9). Instantaneous resistance was determined from the current required to clamp the epithelium to triangle waves of 5 mv amplitude and 40 Hz frequency. Approximate steady-state resistance was calculated from the holding current necessary to maintain a given PD. A transient in this current occurred in the first seconds of clamping as the tubular resistance appeared

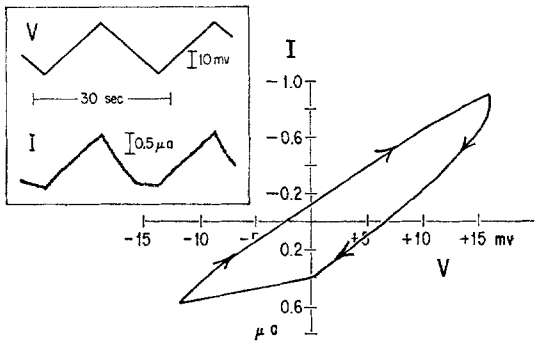

FIGURE 9. *I-V* plot of tubule clamped to low frequency triangle wave voltage command (original current and voltage records shown in *inset*).

to increase approximately threefold from the instantaneous to the steady-state value. Since holding current was not constant, apparent steady-state tubular resistance was calculated from the current required 1 min after the imposition of each holding PD. Table VI summarizes the resistance data; neither steady-state nor instantaneous resistance was significantly related to the holding PD in individual experiments or in the pooled results. Average transepithelial resistance and conductance are presented in Table VII for comparison with resistance and conductance determined from volume flux data of Fig. 8.

DISCUSSION

The experimental focus of the present investigation has been the relation between transepithelial PD and the rate of Na transport in the proximal tubule. The rate of net salt and water transport and the relative magnitudes of the calculated passive fluxes of Na were closely related to the size of the transepithelial PD. A slightly more than twofold increase in the rate of fluid

TABLE VI
TRANSEPITHELIAL RESISTANCE

Holding potential	*R* instantaneous	*R* steady state
mv	*ohm cm²*	*ohm cm²*
−30	15.1±0.14* (2)	100±95 (3)
−25	33.4±24 (9)	158±69 (11)
−20	38.8±24 (9)	158±119 (9)
−15	38.6±24 (12)	120±63 (11)
−10	51.9±33 (11)	158±86 (10)
−5	53.5±41 (5)	95±43 (3)
0	63.6±35 (11)	197±116 (8)
+5	40.5±32 (12)	152±91 (8)
+10	42.1±34 (10)	194±97 (7)
+15	27.7±29 (6)	174±49 (4)
Grand mean	43.2±31 (87)	155.7±89 (75)

Transepithelial electrical resistances were determined as described in the text.
* Mean ± SD, number of observations in parentheses.

TABLE VII
COMPARISON OF EPITHELIAL RESISTANCE AND CONDUCTANCE CALCULATED FROM VOLUME FLUX AND MEASURED ELECTRICALLY

	Volume flux		Electrical current	
	Outward	Inward	Instantaneous	Steady state
R, ohm cm²	620	210	43	156
G, mmho/cm²	1.5	4.8	23.3	6.4

transport by the proximal tubules was observed upon elimination of the transepithelial PD (Table II). From this change in the rate of fluid transport, we calculate a ratio of active to passive Na flux under open-circuit conditions of 1.89. This ratio agrees remarkably well with the value of 1.88 calculated from the data of Boulpaep (17) who used the expanding drop method to determine permeability and unidirectional fluxes. On the basis of the observations of Oken et al. (15), a fourfold increase of net fluid flux would be predicted upon elimination of the transepithelial PD. The flux calculations of Oken et al. were based on a two-compartment model of the proximal tubule; Solomon (20) formulated a three-compartment model and argued that the observations of Oken et al. represented the fluxes across the luminal membrane of the tubule cells rather than true transepithelial fluxes. Since the flux determinations of Oken et al. were based on the disappearance of tracer from the tubule lumen, they were subject to uncertainties introduced by the number of compartments chosen to represent the system and by the possibility of exchange

diffusion. The flux values in the present study were obtained without any assumptions about the nature or number of compartments in the tubule; however, they depend on the assumption that the disappearance of fluid from the tubule lumen is a reflection of its transepithelial movement.

The calculation of the unidirectional fluxes from short-circuited proximal tubules requires the crucial assumption that the active transport rate remains constant as the transepithelial PD is changed over a small range. Information about the relation between active transport rate and transepithelial PD has been obtained in experiments with the isolated frog skin, in which Ussing and Zerahn (21) showed that the active Na flux nearly doubled as the transepithelial PD was reduced from 90 mv to zero. On the other hand, Brinley and Mullins (22) reported that active Na and K fluxes in the squid giant axon were unaffected by changes in membrane potential from 0 to 90 mv. There is, at present, no evidence about the dependence of active Na transport in *Necturus* proximal tubule on the transepithelial PD. In the absence of such evidence, we have assumed a constant active transport rate.

The control fluid reabsorption rates observed in the present study are in agreement with the observations of others. The average intracellular PD of −63 mv is about 10 mv less than the values published by Giebisch (23) and Whittembury and Windhager (24), but agrees well with the value of −61 mv reported by Boulpaep (17). The average free-flow transepithelial PD of −12.6 mv is lower than the value of about −20 mv which has frequently been reported, but is in good agreement with the value of −15.4 mv reported by Boulpaep (17). The 5°–10°C lower body temperature of our animals may be a possible cause for the lower PDs.

In assessing the validity of voltage clamp data, one must consider the type of electrodes used to pass electrical current. In a cylindrical structure such as the proximal tubule, the ideal electrodes for the production of a uniform field are an axial wire and a closely approximated circumferential coil (25). In the present experiments, a circumferential coil was neither feasible nor necessary since the electrode system used may be shown by electrostatic theory to produce a uniform field with less than 0.1% variation in PD across the entire luminal surface of the epithelium. Errors in the determination of PD caused by the resistance of nonepithelial elements between the potential and indifferent electrodes are also insignificant (less than 1%). Adequate voltage clamping of a substantial length of tubule from a point source of current, e. g., a glass microelectrode, is virtually impossible in most cylindrical cables (including proximal tubule) from geometric considerations alone. In addition, electrical current data from voltage clamp experiments are of limited value unless they can be related to ionic currents. Ideally, voltage clamp analysis should employ an independent measure of ionic flux.

Previous attempts at voltage clamping renal tubules have been limited to

passage of current from glass microelectrodes inserted into the tubular lumen for the purpose of eliminating the spontaneous, transepithelial PD. Simultaneous flux determinations were not carried out because of the limited size of the tubular segments subjected to clamping. Eigler (16) eliminated the proximal tubular transepithelial PD by passage of current from a glass microelectrode placed in a split droplet of a *Necturus* nephron. Cable properties limited the size of clamped droplets to two tubular diameters; "short-circuit current" so obtained was not significantly different from the net Na flux of the split drop experiments of Whittembury et al. (19). Windhager and Giebisch (26) reported similar results from short-circuit experiments in split droplets of the rat proximal tubule.

The short-circuit experiments of previous investigators (16, 26) were hampered not only by technical problems concerning the uniformity of the electrical field, but also by theoretical considerations which necessitate knowledge of both the shunt resistance and the influence of tubular topology on the electric field produced (2). Extracellular shunt resistance is now known to be very low (17), and most of the SCC would be expected to bypass the cells. Since the shunt resistance is the predominant factor in the low transepithelial resistance, it is worth noting that the instantaneous transepithelial resistance in Table VI does not change significantly under short-circuit conditions. The presence of an axial electrode in the tubular lumen removes the limitations imposed by the tubular space constant which hampered earlier investigations. Since chloride transport in the *Necturus* proximal tubule has been shown to be passive (27) it would not be expected to influence the SCC-Na flux relationship. While the apparent SCC was not significantly different from the net flux (Table IV), the variability of the electrical data makes an exact relationship between flux and current difficult to establish. However, the above factors do not influence the Na pump rate calculated from the observed fluid transport in the absence of a transepithelial PD. The slow generation of acid (HCl or hypochlorite) at the anode and base (NaOH) at the cathode of the platinized electrodes did not seem to interfere with tubular function since flux rate and PD returned to control values after each clamping period. The buffering capacity of the tubular and extracellular fluids, together with the relative rapidity of ionic movements in this system, probably combined to minimize pH changes.

The transepithelial resistance is a variable of major importance in the evaluation of the functional properties of *Necturus* proximal tubular epithelium, since it gives an indication of the pathways and mechanisms for fluid movement. Windhager et al. (28) reported a transepithelial resistance of 650 Ω cm^2, based on current-voltage records obtained with double-barrel microelectrodes. They reasoned that since this resistance was only $\frac{1}{10}$ or less of the resistance of the individual cell membranes, significant paracellular shunting must occur. Boulpaep in turn suggested that their transepithelial resistance value was it-

self too high by a factor of 10 and determined from cable analysis that the tubular epithelium behaved as an ohmic resistor of 70 Ω cm^2 (17). The low values of transepithelial resistance in Table VI as well as the observations of previous investigators support the conclusion that transepithelial ionic movements occur principally through extracellular pathways.

Steady-state and instantaneous resistances determined by triangle wave voltage clamp appear to be relatively constant and unrelated to the value of the holding potential (Table VI). Yet the low frequency triangle wave clamps result in hysteresis, a fact which suggests that transepithelial resistance or spontaneous PD may be altered by changes in holding PD (Fig. 9). The major part of the apparent increase in effective transepithelial resistance which occurs during prolonged clamps may be related to changes in spontaneous PD induced by current passage. As current passage continues, the spontaneous transepithelial PD moves toward the holding potential, reducing the current necessary to maintain the holding potential and increasing the calculated resistance. Changes in spontaneous PD are presumably "polarization PDs" consequent to changes in the concentration of electrolytes in the intercellular spaces of the tubular epithelium (18).

Several points in the relationship between net fluid or Na flux and transepithelial PD, presented in Fig. 8, warrant consideration. Net fluid movement takes place in the same direction as net cation movement. Passive movement of fluid towards the negative electrode during the passage of current may be due to electro-osmosis or to the alteration of intraepithelial solute concentrations, which may manifest itself by the appearance of a voltage transient after cessation of current passage (Fig. 7). The presence of such a transient is an important observation favoring concentration-induced fluid movement rather than electroosmotic fluid flow. It is consistent with the relaxation of a concentration gradient in an unstirred layer and suggests that current passage induces changes in the concentration of electrolytes within the epithelium (18).

The Na (or fluid) fluxes per unit driving force exhibit marked asymmetry depending on the direction of net fluid movement (Fig. 8). Such asymmetry or rectification of fluid fluxes suggests different pathways for transepithelial fluid flow, or changes in epithelial Na permeability, depending on the direction of net fluid flux or on the transepithelial PD. Rectification of fluid movement was predicted in two-membrane model systems (29), and observed in osmotic flow in *Necturus* proximal tubule. The hydraulic conductivity of the *Necturus* proximal tubule was greater when the osmotically induced water flux occurred from lumen to plasma than it was when the flux was in the opposite direction (6), whereas our observations suggest a greater fluid flux per millivolt for flow from plasma to lumen than in the opposite direction.

Finally, Fig. 8 was used to calculate the epithelial permeability to Na; dif-

ferent values were obtained, depending on the method of calculation. All of the values were derived from the Goldman-Hodgkin-Katz equation and therefore assume a constant electrical field within the tubular epithelium. Permeability should ideally be calculated in the absence of net fluid movement to minimize the effect of solvent drag on ionic fluxes. This condition is fulfilled at -15 mv, the flux equilibrium point, at which passive flux from plasma to lumen, driven by the transepithelial PD, must equal the active flux from lumen to plasma. The exact values of the individual fluxes are not known, and they were both assumed to be equal to the active flux measured at zero PD (227 pmoles/cm^2 per sec), leading to a calculated permeability of 7.05×10^{-6} cm/sec. The slope of the flux-potential line in the range -15 to $+10$ mv was also used to calculate a permeability value, 3.73×10^{-6} cm/sec, which is somewhat smaller than that determined at flux equilibrium, possibly as a consequence of the solvent drag effects of net fluid movement in the direction lumen to plasma.

The observations reported here lend support to many features of the current model of fluid transport in the proximal tubule (7, 18). The existence of a low transepithelial resistance relative to individual cell membrane resistance has been substantiated. In addition, the linear instantaneous current-voltage characteristics of the epithelium suggest the passage of current through a "thick" barrier, such as the tight junction, rather than through a "thin" barrier like a cell membrane (30). The observed voltage transients and current hysteresis are consistent with the development of a local osmotic gradient within the epithelium. The existence of opposing unidirectional fluxes of greater magnitude than the net flux has been substantiated by a method free of the complications of tracer analysis. Together these observations constitute a strong argument for the transepithelial passage of ionic species through extracellular pathways and for the importance of those sites in the generation of the transepithelial potential difference.

The present investigation has established experimentally the important influence of the transepithelial PD on fluid movement in the proximal tubule. The possibility that changes in PD might play a role in the normal control of net fluid transport has not been considered heretofore, although it is a logical consequence of the high ionic and water permeability of the tubular epithelium.

The authors wish to thank Dr. Barbara Howell for performing the measurements of pH.
A portion of this investigation is based on a dissertation submitted by Kenneth R. Spring to the faculty of the State University of New York at Buffalo in partial fulfillment of the requirements for a Ph.D.
Kenneth R. Spring was supported in part by National Institutes of Health Fellowship 1-F02-DE44102-01A1 from the National Institutes of Dental Research.

Received for publication 9 November 1971.

REFERENCES

1. WILBRANDT, W. 1938. Electrical potential differences across the wall of kidney tubules of *Necturus*. *J. Cell. Comp. Physiol.* **11**:425.
2. WINDHAGER, E. E., and G. GIEBISCH. 1965. Electrophysiology of the nephron. *Physiol. Rev.* **45**:214.
3. HOWELL, B. J., F. W. BAUMGARDNER, K. BONDI, and H. RAHN. 1970. Acid-base balance in cold-blooded vertebrates as a function of body temperature. *Am. J. Physiol.* **218**: 600.
4. WINDHAGER, E. E. 1968. Micropuncture Techniques and Nephron Function. Appleton-Century-Crofts Inc., New York. 10.
5. GERTZ, K. H. 1963. Transtubuläre Natriumchloridflüsse und Permeabilität für Nichtelektrolyte im proximalen und distalen Konvolut der Rattenniere. *Pfluegers Arch. Gesamte Physiol. Menschen Tiere.* **276**:336.
6. BENTZEL, C. J., B. PARSA, and D. K. HARE. 1969. Osmotic flow across proximal tubule of *Necturus*. Correlation of physiologic and anatomic studies. *Am. J. Physiol.* **217**:570.
7. GIEBISCH, G. 1961. Measurements of electrical potential differences on single nephrons of the perfused *Necturus* kidney. *J. Gen. Physiol.* **44**:659.
8. COLE, K. S., and U. KISHIMOTO. 1962. Platinized silver chloride electrode. *Science* (*Wash. D.C.*). **136**:381.
9. MOORE, J. W., and K. S. COLE. 1963. Voltage clamp techniques. *Phys. Tech. Biol. Res.* **6**(B):263.
10. NAKAJIMA, K., J. R. CLAPP, and R. R. ROBINSON. 1970. Limitations of the shrinking-drop micropuncture technique. *Am. J. Physiol.* **210**:345.
11. GOLDMAN, D. E. 1943. Potential, impedance, and rectification in membranes. *J. Gen. Physiol.* **27**:37.
12. Hodgkin, A. L., and B. KATZ. 1949. The effect of sodium ions on the electrical activity of the giant axon of the squid. *J. Physiol.* (*Lond.*). **108**:37.
13. BENTZEL, C. J., T. ANAGNOSTOPOULOS, and H. PANDIT. 1970. *Necturus* kidney: its response to effects of isotonic volume expansion. *Am. J. Physiol.* **218**:205.
14. SCOTT, W. N., D. L. MAUDE, I. SHEHADEH, and A. K. SOLOMON. 1966. Transtubular movement of albumin in *Necturus* kidney. *Am. J. Physiol.* **211**:1039.
15. OKEN, D. E., G. WHITTEMBURY, E. E. WINDHAGER, and A. K. SOLOMON. 1963. Single proximal tubules of *Necturus* kidney. V. Unidirectional sodium movement. *Am. J. Physiol.* **204**:372.
16. EIGLER, F. W. 1961. Short-circuit current measurements in proximal tubule of *Necturus* kidney. *Am. J. Physiol.* **201**:157.
17. BOULPAEP, E. L. 1972. Permeability changes of the proximal tubule of *Necturus* during saline loading. *Am. J. Physiol.* **222**:517.
18. WEDNER, H. J., and J. D. DIAMOND. 1969. Contributions of unstirred-layer effects to apparent electrokinetic phenomena in the gall bladder. *J. Membrane Biol.* **1**:92.
19. WHITTEMBURY, G., N. SUGINO, and A. K. SOLOMON. 1961. Ionic permeability and electrical potential difference in *Necturus* kidney cells. *J. Gen. Physiol.* **44**:689.
20. SOLOMON, A. K. 1963. Single proximal tubules of *Necturus* kidney. VII. Ion fluxes across individual faces of cell. *Am. J. Physiol.* **204**:381.
21. USSING, H. H., and K. ZERAHN. 1951. Active transport of sodium as the source of electric current in the short-circuited isolated frog skin. *Acta Physiol. Scand.* **23**:110.
22. BRINLEY, F. J., and L. J. MULLINS. 1971. The fluxes of sodium and potassium across the squid axon membrane under conditions of altered membrane potential. *Fed. Proc.* **30**: 255.
23. GIEBISCH, G. 1958. Electrical potential measurements on single nephrons of *Necturus*. *J. Cell. Comp. Physiol.* **51**:221.
24. WHITTEMBURY, G., and E. E. WINDHAGER. 1961. Electrical potential difference measurements in perfused single proximal tubules of *Necturus* kidney. *J. Gen. Physiol.* **44**:679.

25. COLE, K. S. 1968. Membranes, Ions and Impulses. University of California Press, Berkeley, Calif. 241–269.
26. WINDHAGER, E. E., and G. GIEBISCH. 1961. Comparison of short-circuit current and net water movement in single perfused proximal tubules of rat kidneys. *Nature (Lond.)*. **191**:1205.
27. GIEBISCH, G., and E. E. WINDHAGER. 1963. Measurement of chloride movement across single proximal tubules of *Necturus* kidney. *Am. J. Physiol.* **204**:387.
28. WINDHAGER, E. E., E. L. BOULPAEP, and G. GIEBISCH. 1967. Electrophysiological studies on single nephrons. *Proc. Int. Congr. Nephrol.* **1**:35.
29. PATLAK, C. S., D. A. GOLDSTEIN, and J. F. HOFFMAN. 1963. The flow of solute and solvent across a two-membrane system. *J. Theor. Biol.* **5**:426.
30. WRIGHT, E. M., P. H. BARRY, and J. M. DIAMOND. 1971. The mechanism of cation permeation in rabbit gallbladder. *J. Membrane Biol.* **4**:331.